

A General Approach to Ammann Bars for Aperiodic Tilings

Thomas Fernique* Carole Porrier†

Abstract

Ammann bars are formed by segments (decorations) on the tiles of a tiling such that forming straight lines with them while tiling forces non-periodicity. Only a few cases are known, starting with Robert Ammann's observations on Penrose tiles, but there is no general explanation or construction. In this article we propose a general method for cut and project tilings based on the notion of *subperiods* and we illustrate it with an aperiodic set of 36 decorated prototiles related to what we called *Cyrenaic tilings*.

1 Introduction

Shortly after the famous Penrose tilings were introduced by Roger Penrose in 1974 [Pen74] and popularized by Martin Gardner in 1977 [Gar77], amateur mathematician Robert Ammann [Sen04] found particularly interesting decorations of the tiles (Figure 1): if one draws segments in the same way on all congruent tiles then on any valid tiling then all those segments compose straight lines, going in five different directions. Conversely if one follows the assembly rule consisting of prolonging every segment on the tiles into a straight line then the obtained tiling is indeed a Penrose tiling. Those lines are called *Ammann bars*.

Penrose tilings have many interesting properties and can be generated in several ways. The cut and project method follows their algebraic study by de Bruijn in 1981 [dB81]. Beenker soon proposed a whole family of tilings based on it [Bee82], including the Ammann-Beenker tilings that Ammann found independently. A cut and project tiling can be seen as a digitization of a two-dimensional plane in a n -dimensional Euclidean space ($n > 2$), and we will talk about $n \rightarrow 2$ *tilings* in that sense. When the *slope* of the plane does not contain any rational line, the tiling is non-periodic. This is the case for Penrose tilings for instance, so the set of tiles defining them is *aperiodic*: one can tile the plane with its tiles but only non-periodically. The first aperiodic tileset was found by Berger, thus proving the undecidability of the *Domino Problem* [Ber66]

*Université Sorbonne Paris Nord and CNRS

†Université du Québec à Montréal and Université Sorbonne Paris Nord

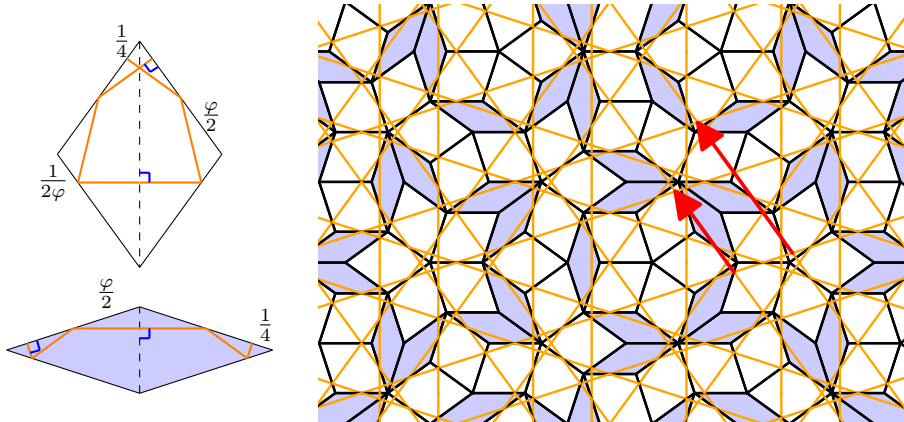


Figure 1: Left: Penrose tiles with Ammann segments (in orange). On each rhombus the dashed line is an axis of symmetry and the sides have length $\varphi = (1 + \sqrt{5})/2$. Right: Ammann bars on a valid pattern of Penrose tiles, where each segment is correctly prolonged on adjacent tiles. The red vectors are “integer versions” of one subperiod.

and relating tilings to logic. Since then, relatively few others were exhibited: many non-periodic tilings exist (even infinitely many using the cut and project method), but we usually do not have a corresponding aperiodic tileset.

Links were made between such tilings and quasicrystals [Sen95, SO87], that is crystals whose diffraction pattern is not periodic but still ordered, with rotational symmetries. The study of *local rules*, i.e. constraints on the way tiles can fit together in finite patterns, can help modeling the long range aperiodic order of quasicrystals. For instance, Penrose tilings are defined by their 1-*atlas*, which is a small number of small patterns: any and all tilings containing only those patterns (of the given size) are Penrose tilings. Alternately, they can also be defined by their *Ammann local rules*, as stated in the first paragraph. On the contrary, it was proven [Bur88, BF15a] that Ammann-Beenker tilings, also known as 8-fold tilings, do not have *weak local rules*, i.e. no finite set of patterns is enough to characterize them. Socolar found sort of Ammann bars for them [Soc89], but they extend outside the boundary of the tiles, thus do not fit the framework considered here.

Grünbaum and Shephard [GS87] detail the properties of Ammann bars in the case of Penrose tilings and their close relation to the *Fibonacci word*. They also present two tilesets by Ammann with Ammann bars but these are substitutive and not cut and project tilings. Generally speaking, we do not know much about Ammann bars and for now each family of aperiodic tilings has to be observed as an example. Yet they can reveal quite useful to study the structure of tilings, and were used by Porrier and Blondin Massé [PBM20] to solve a combinatorial optimization problem on graphs defined by Penrose tilings.

Here, we would like to find necessary and/or sufficient conditions for a family

of tilings to have Ammann bars. When it comes to $4 \rightarrow 2$ tilings (digitizations of planes in \mathbb{R}^4) and a few others like Penrose, which are $5 \rightarrow 2$ tilings, the existence of weak local rules can be expressed in terms of *subperiods*, which are particular vectors of the slope [BF15b, BTh17]. As mentioned above, Ammann-Beenker tilings have no local rules and their slope cannot be characterized by its subperiods. Careful observation of Penrose tilings from this angle shows that Ammann bars have the same directions as subperiods: there are two subperiods in each direction, one being φ times longer than the other. Additionally, the lengths of the “integer versions” of subperiods are closely related to the distances between two consecutive Ammann bars in a given direction, as can be seen in Figure 1 (some details are given in Appendix A). Though interesting, this special case is too particular to hope for a generalization from it alone. Nonetheless, we think that Ammann bars are related to subperiods.

Since subperiods are simpler for $4 \rightarrow 2$ tilings, for which we also have a stronger result regarding weak local rules, we focus on those. Namely, Bédaride and Fernique [BTh17] showed that a $4 \rightarrow 2$ tiling has weak local rules if and only if its slope is characterized by its subperiods. It seems some conditions of alignment play a part in the existence of Ammann bars. This led us to introduce the notion of *good projection* (Def. 1 p. 9) on a slope, which plays a prominent role in our method to define Ammann bars. Thus we conjecture the following:

Conjecture 1 *If a $4 \rightarrow 2$ tiling admits weak local rules and a good projection, then it admits Ammann local rules.*

We propose a constructive method to find Ammann bars for $4 \rightarrow 2$ tilings which are characterized by subperiods and for which we can find a good projection. We found several examples of slopes respecting the conditions. Among those, we focused on a slope based on the irrationality of $\sqrt{3}$, defining tilings that we called *Cyrenaic tilings* in reference to Theodorus of Cyrene who proved $\sqrt{3}$ to be irrational. They have “short” subperiods, which facilitates observations on drawings. From those tilings, we constructed the set of decorated tiles in Figure 2. Those tiles give Ammann bars to Cyrenaic tilings and we show the following:

Theorem 1 *The tileset \mathcal{C} in Figure 2 is aperiodic.*

Some of our results hold for any $4 \rightarrow 2$ tiling respecting the conditions above. We conjecture that our method is general, though for now we do not know how to prove that the obtained tileset is necessarily aperiodic. The case of Penrose indicates that our method could (and should) be adapted in order to work for $5 \rightarrow 2$ tilings, or general cut and project ($n \rightarrow d$) tilings. In particular, for Penrose the lines are shifted and the number of lines is reduced compared with our method, so that only two decorated tiles are needed. Besides, in each direction the distance between two consecutive lines can take only two values, and the sequence of intervals is substitutive. In the case of Cyrenaic tilings, the bi-infinite word defined by each sequence of intervals between Ammann bars seems to be substitutive so maybe we could compose them after finding the

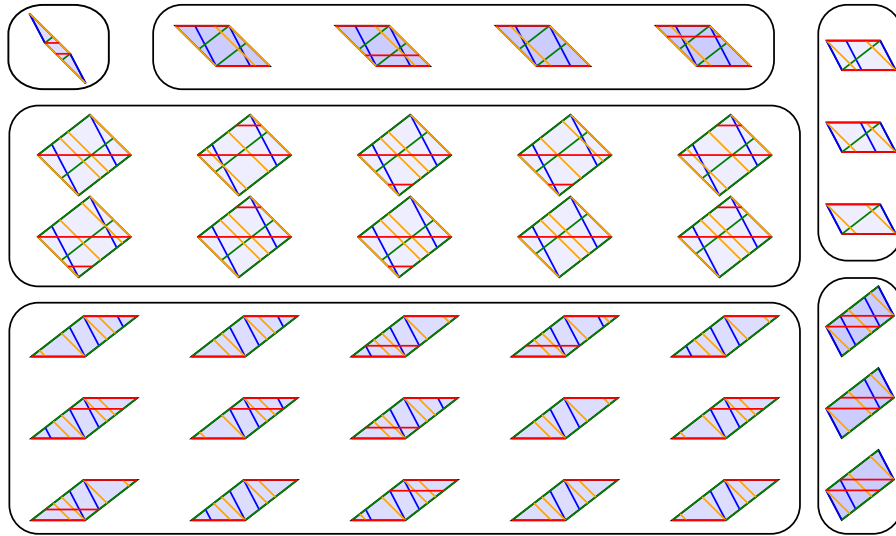


Figure 2: Set \mathcal{C} of 36 decorated prototiles obtained from Cyrenaic tilings. Any tiling by these tiles where segments extend to lines (Ammann local rules) is non-periodic (Th. 1).

substitution. Lines could also be shifted as it is the case for Penrose tilings, instead of passing through vertices. An optimal shift (reducing the number of lines or tiles) would then have to be determined.

The paper is organized as follows. Section 2 introduces the settings, providing the necessary formal definitions, in particular local rules and subperiods. In Section 3 we present our method to construct a set of decorated prototiles yielding Ammann bars. We rely on subperiods characterizing a slope as well as a good projection. General results regarding $4 \rightarrow 2$ tilings are proven. Finally, in Section 4 we show that Ammann bars of the set \mathcal{C} force any tiling with its tiles to have the same subperiods as Cyrenaic tilings, thus proving Theorem 1.

2 Settings

2.1 Canonical cut and project tilings

A **tiling** of the plane is a covering by **tiles**, that is compact subsets of the space, whose interiors are pairwise disjoint. Here we focus on **tilings by parallelograms**: let v_0, \dots, v_{n-1} ($n \geq 3$) be pairwise non-collinear vectors of the Euclidean plane, they define $\binom{n}{2}$ parallelogram *prototiles* which are the sets $T_{ij} := \{\lambda v_i + \mu v_j \mid 0 \leq \lambda, \mu \leq 1\}$; then the tiles of a tiling by parallelograms are translated prototiles (tile rotation or reflection is forbidden), satisfying the edge-to-edge condition: the intersection of two tiles is either empty, a vertex or

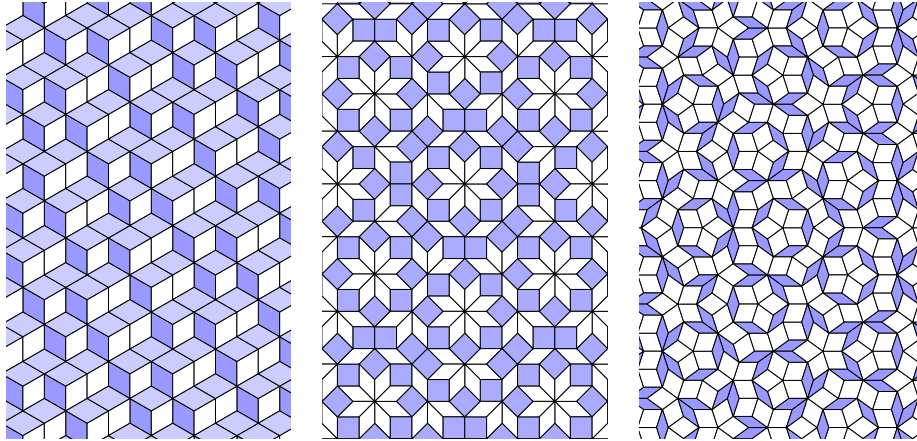


Figure 3: Examples. Left: Rauzy tiling from which you can visualize the lift in \mathbb{R}^3 . Center: Ammann-Beenker tiling. Right: Penrose tiling.

an entire edge. When the v_i 's all have the same length, such tilings are called *rhombus tilings*.

Let e_0, \dots, e_{n-1} be the canonical basis of \mathbb{R}^n . Following Levitov [Lev88] then Bédaride and Fernique [BF15b], a tiling by parallelograms can be **lifted** in \mathbb{R}^n , to correspond with a “stepped” surface of codimension $n - 2$ in \mathbb{R}^n , which is unique up to the choice of an initial vertex. An arbitrary vertex is first mapped onto the origin, then each tile of type T_{ij} is mapped onto the 2-dimensional face of a unit hypercube of \mathbb{Z}^n generated by e_i and e_j , such that two tiles adjacent along an edge v_i are mapped onto two faces adjacent along an edge e_i . This is particularly intuitive for $3 \rightarrow 2$ tilings which are naturally seen in 3 dimensions (Fig. 3, left). The principle is the same for larger n , though difficult to visualize.

If a tiling by parallelograms can be lifted into a tube $E + [0, t]^n$ where $E \subset \mathbb{R}^n$ is a plane and $t \geq 1$, then this tiling is said to be **planar**. In that case, **thickness** of the tiling is the smallest suitable t , and the corresponding (unique up to translation) E is called the **slope** of the tiling. A planar tiling by parallelograms can thus be seen as an approximation of its slope, which is as good as the thickness is small. Planarity is said **strong** if $t = 1$ and **weak** otherwise.

Strongly planar tilings by parallelograms can also be obtained by the so-called **(canonical) cut and project method**. For this, consider a d -dimensional affine plane $E \subset \mathbb{R}^n$ such that $E \cap \mathbb{Z}^n = \emptyset$, select (“cut”) all the d -dimensional facets of \mathbb{Z}^n which lie within the tube $E + [0, 1]^n$, then “project” them onto \mathbb{R}^d . If this projection π yields a tiling of \mathbb{R}^d it is called **valid** (see Figure 4), and the tiling is a strongly planar tiling by parallelograms with slope E . Such tilings are called canonical cut and project tilings or simply **$n \rightarrow d$ tilings**. Not every projection is suitable, but the orthogonal projection onto E seen as \mathbb{R}^d is known to be valid [Har04]. Here we only consider the case of a 2-dimensional

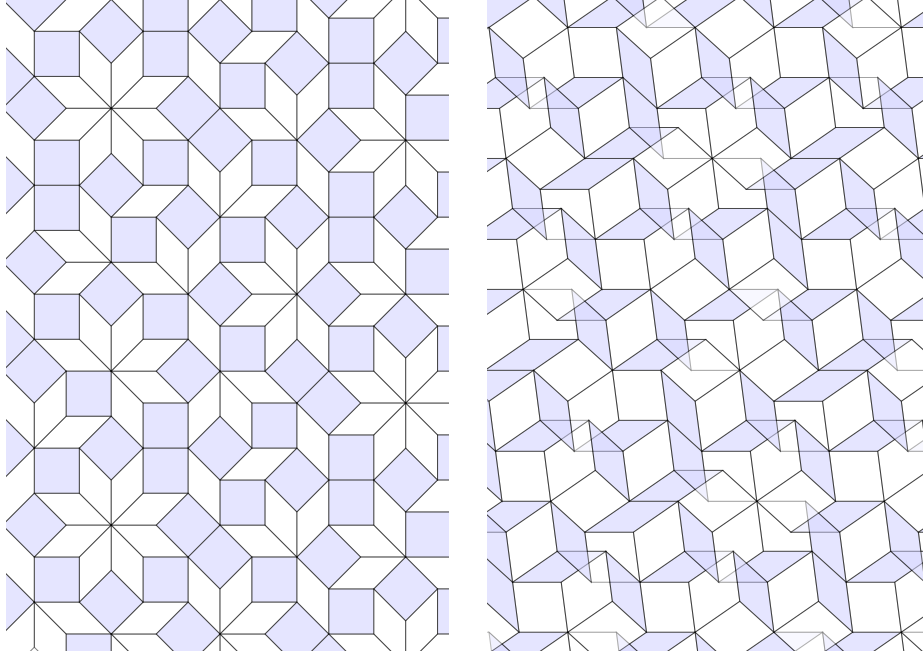


Figure 4: Golden octagonal tiling with the usual valid projection (left) and a non-valid projection on the same slope (right). Colors of the tiles are the same with respect to the $\pi(e_i)$'s, with an opacity of 50% in both images.

slope E which is totally irrational, that is, which does not contain any rational line. This yields aperiodic tilings of the plane.

Figure 3 illustrates the above notions with three well-known examples. Rauzy tilings are $3 \rightarrow 2$ tilings whose slope E is generated by

$$\vec{u} = (\alpha - 1, -1, 0) \quad \text{and} \quad \vec{v} = (\alpha^2 - \alpha - 1, 0, -1),$$

where $\alpha \approx 1.89$ is the only real root of $x^3 - x^2 - x - 1$. Ammann-Beenker tilings, composed of tiles of the set A5 in the terminology of Grünbaum and Shephard [GS87], are the $4 \rightarrow 2$ tilings with slope E generated by

$$\vec{u} = (\sqrt{2}, 1, 0, -1) \quad \text{and} \quad \vec{v} = (0, 1, \sqrt{2}, 1).$$

Generalized Penrose tilings are the $5 \rightarrow 2$ tilings with slope E generated by

$$\vec{u} = (\varphi, 0, -\varphi, -1, 1) \quad \text{and} \quad \vec{v} = (-1, 1, \varphi, 0, -\varphi),$$

where $\varphi = (1 + \sqrt{5})/2$ is the golden ratio. The “strict” Penrose tilings as defined by Roger Penrose in [Pen78] (set P3 in the terminology of [GS87]) corresponds to the case when E contains a point whose coordinates sum to an integer.

2.2 Local rules

Local rules for tilings can be defined in several ways, which are not equivalent. Since we focus on cut and project tilings, we also define local rules for a slope.

Firstly, weak local rules for a tiling T can be defined as in [BF15b]. A **pattern** is a connected finite subset of tiles of T . Following [Lev88], an **r-map** of T is a pattern formed by the tiles of T which intersect a closed disk of radius $r \geq 0$. The **r-atlas** of T , denoted by $T(r)$, is then the set of all r -maps of T (up to translation). In the case of a canonical cut and project tiling, it is a finite set. A canonical cut and project tiling \mathcal{P} of slope E is said to admit **weak local rules** if there exist $r \geq 0$ and $t \geq 1$, respectively called **diameter** and **thickness**, such that any $n \rightarrow d$ tiling T whose r -atlas is contained in $\mathcal{P}(r)$ is planar with slope E and thickness at most t . By extension, the slope E is then said to admit local rules. In that case, we say that the slope of \mathcal{P} is characterized by its patterns of a given size. Local rules are **strong** if $t = 1$. Penrose tilings have strong local rules and the slope is characterized by patterns of the 1-atlas if the sides of the tiles have length 1 (see [Sen95], Theorem 6.1, p.177).

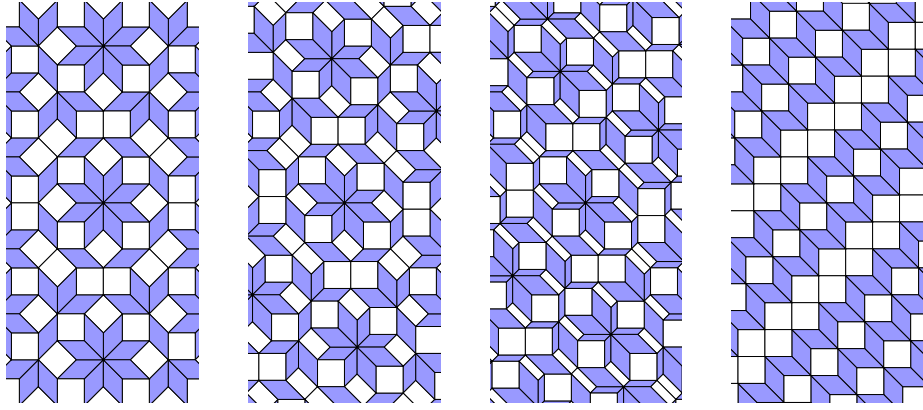
Another way of defining local rules is with Ammann bars. We call **Ammann segments** decorations on tiles which are segments whose endpoints lie on the borders of tiles, such that when tiling with those tiles, each segment has to be continued on adjacent tiles to form a straight line. We say that a slope E admits **Ammann local rules** if there is a finite set of prototiles decorated with Ammann segments such that any tiling with those tiles is planar with slope E . In particular, no periodic tiling of the plane should be possible with those tiles if E is irrational. For instance, the marking of the Penrose tiles yielding Ammann bars is shown in Figure 1, along with a valid pattern where each segment is correctly prolonged on adjacent tiles.

2.3 Subperiods

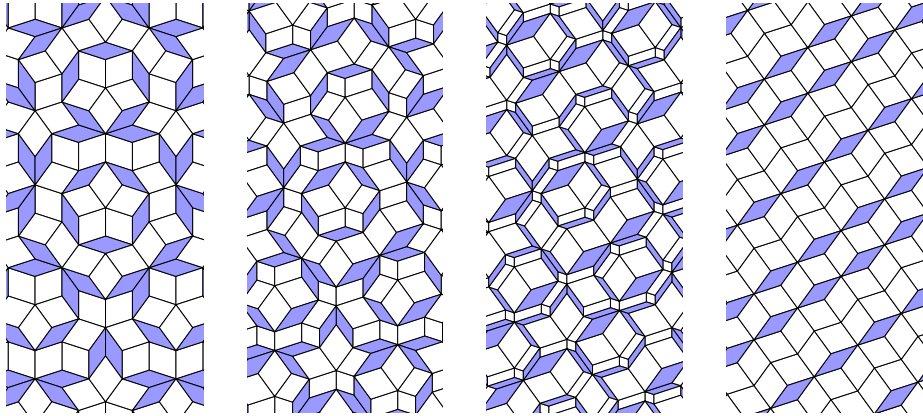
Adapted from Bédaride and Fernique [BF13], the i_1, \dots, i_{n-3} -**shadow** of an $n \rightarrow 2$ tiling T is the orthogonal projection $\pi_{i_1, \dots, i_{n-3}}$ of its lift on the space generated by $\{e_j \mid 0 \leq j \leq n-1, j \neq i_1, \dots, i_{n-3}\}$. This corresponds to reducing to zero the lengths of $\pi(e_{i_1}), \dots, \pi(e_{i_{n-3}})$ in the tiling, so that the tiles defined by these vectors disappear. This is illustrated in Figure 5.

An $n \rightarrow 2$ tiling thus has $(n3)$ shadows.

An i_1, \dots, i_{n-3} -**subperiod** of an $n \rightarrow 2$ tiling T is a prime period of its i_1, \dots, i_{n-3} -shadow, hence an integer vector in \mathbb{R}^3 . By extension, we call subperiod of a slope E any vector of E which projects on a subperiod in a shadow of T . A subperiod is thus a vector of E with 3 integer coordinates: those in positions $j \notin \{i_1, \dots, i_{n-3}\}$. We say that a slope is *determined* or *characterized* by its subperiods if only finitely many slopes have the same subperiods. For



(a) Starting from an Ammann-Beenker tiling (on the left), progressively reduce the length of one of the four vectors defining the tiles, until it is null (on the right). The shadow thus obtained is periodic in one direction.



(b) Starting from a Penrose tiling (on the left), progressively reduce the lengths of two of the five vectors defining the tiles, until they are null (on the right). The shadow thus obtained is periodic in one direction.

Figure 5: Shadows of Ammann-Beenker and Penrose tilings.

instance, the slope of Ammann-Beenker tilings has four subperiods:

$$\begin{aligned}
 p_0 &= (\sqrt{2}, 1, 0, -1), \\
 p_1 &= (1, \sqrt{2}, 1, 0), \\
 p_2 &= (0, 1, \sqrt{2}, 1), \\
 p_3 &= (-1, 0, 1, \sqrt{2}).
 \end{aligned}$$

while that of Penrose tilings has ten, each with two non-integer coordinates (Appendix A).

This notion was first introduced by Levitov [Lev88] as the *second intersection condition* and then developed by Bédaride and Fernique, who showed in [BF15b] and [BTh17] that in the case of $4 \rightarrow 2$ tilings, a plane admits weak local rules if and only if it is determined by its subperiods. It was shown in [BF13] that this is not the case for Ammann-Beenker tilings: indeed, their subperiods are the same for all Beenker tilings (introduced in [Bee82]), that are the planar tilings with a slope generated, for any $s \in (0, \infty)$, by

$$u = (1, 2/s, 1, 0) \quad \text{and} \quad v = (0, 1, s, 1).$$

The Ammann-Beenker tilings correspond to the case $s = \sqrt{2}$ and do not admit local rules [Bur88, BF15a]. On the other hand, generalized Penrose tilings have a slope characterized by its subperiods [BF15b] and do admit local rules.

In this article, we focus on $4 \rightarrow 2$ tilings with irrational slope E . In this case, each subperiod of E has exactly one non-integer coordinate. Since the vertices of the tiling are projected points of \mathbb{Z}^4 , we define “integer versions” of subperiods: if $p_i = (x_0, x_1, x_2, x_3)$ is a subperiod, then its floor version is $\lfloor p_i \rfloor = (\lfloor x_0 \rfloor, \lfloor x_1 \rfloor, \lfloor x_2 \rfloor, \lfloor x_3 \rfloor)$ and its ceil version is $\lceil p_i \rceil = (\lceil x_0 \rceil, \lceil x_1 \rceil, \lceil x_2 \rceil, \lceil x_3 \rceil)$. Note that only the non-integer coordinate x_i is affected, and that $\lfloor p_i \rfloor, \lceil p_i \rceil \notin E$.

3 Cyrenaic tilings and Ammann bars

In this section, we present a construction to get Ammann bars for some $4 \rightarrow 2$ tilings and we give the example of what we named *Cyrenaic tilings*.

3.1 Good projections

In Subsection 2.1, we defined what is a valid projection for a slope E and mentioned the classical case of the orthogonal projection. There are however other valid projections, and this will play a key role here. We will indeed define Ammann bars as lines directed by subperiods and it will be convenient for the projected i -th subperiod $\pi(p_i)$ to be collinear with $\pi(e_i)$, so that the image of a line directed by p_i is still a line in the i -th shadow (Figure 6). This leads us to introduce the following definition:

Definition 1 A **good projection** for a 2-dimensional slope $E \subset \mathbb{R}^4$ is a valid projection $\pi : \mathbb{R}^4 \rightarrow \mathbb{R}^2$ such that for every $i \in \{0, 1, 2, 3\}$, $\pi(p_i)$ and $\pi(e_i)$ are collinear.

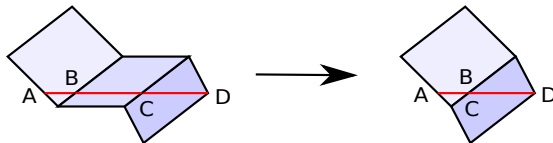


Figure 6: Aligned segments in a pattern remain aligned in the shadow corresponding to the direction of the line.

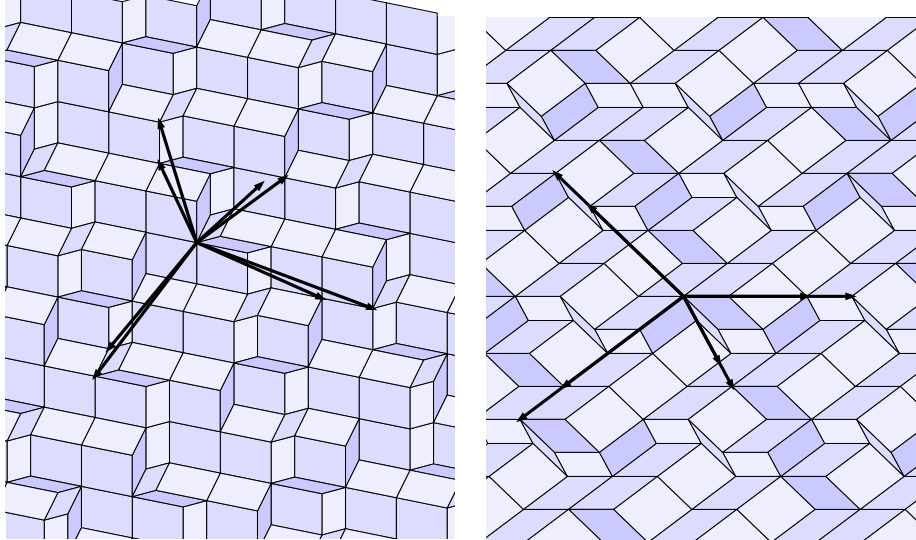


Figure 7: Cyrenaic tiling with $\pi(\lfloor p_i \rfloor)$ and $\pi(\lceil p_i \rceil)$ for each subperiod p_i . On the left, we used the orthogonal projection which is valid but not *good*; on the right we used a good projection. Colors of the tiles are the same on both images with respect to the $\pi(e_i)$'s. Starting from the central pattern, one can see how one tiling is just a deformation of the other.

Figure 7 illustrates the difference between two valid projections, one being good but not the other, on the slope of Cyrenaic tilings which we present in the next subsection. With the good projection, projected subperiods have the same directions as the sides of the tiles. This is why if segments on the tiles of a tiling T are directed by $\pi(p_i)$ then continuity of the lines in direction i is preserved in the i -shadow of T , for any $i \in \{0, 1, 2, 3\}$, as illustrated in Figure 6. Indeed, consider a line L in direction i , then it is parallel to the sides of the tiles which disappear in the i -shadow of T . Now consider a tile t_0 which disappears in this shadow, containing a segment $[BC] \subset L$, and its neighbors t_{-1} and t_1 containing segments $[AB], [CD] \subset L$. Taking the i -shadow corresponds to translating remaining tiles in direction i , hence by such a translation the endpoint of an Ammann segment is mapped to a point on the same line (namely the image of the other endpoint of the same segment). As a result, the images of points B and C are on the same line, so that points A, B, C, D are still aligned.

3.2 Finding good projections

Given a slope E with subperiods p_0, \dots, p_3 , we search for a good projection π as follows. We will define it by its 2×4 matrix A , which must satisfy $Ae_i = \lambda_i Ap_i$ for $i = 0, \dots, 3$, where $\Lambda := (\lambda_i)_{i=0, \dots, 3}$ is to be determined. With M denoting the 4×4 matrix whose i -th column is $e_i - \lambda_i p_i$, this rewrites $AM = 0$. The 2

rows of A must thus be in the left kernel of M . Since the image of the facets in $E + [0, 1]^4$ must cover \mathbb{R}^2 , A must have rank 2. Hence the left kernel of M must be of dimension at least 2, that is, M must have rank at most 2. This is equivalent to saying that all the 3×3 minors of M must be zero. Each minor yields a polynomial equation in the λ_i 's. Any solution of the system formed by these equations yields a matrix M whose left kernel can be computed. If the kernel is not empty, then any basis of it yields a suitable matrix A .

Of course with 4 variables and 16 equations there is no guarantee that a solution exists, and oftentimes when a projection respects the collinear condition in Definition 1 it is not valid: some tiles are superimposed in what should be a tiling. Figure 4 shows for instance what happens in the case of golden octagonal tilings (introduced in [BF15b]) when the obtained matrix A is used. To find a slope E with a good projection, we proceed as follows:

1. Randomly choose the three integer coordinates of each subperiod p_i ;
2. Check that only finitely many slopes admit these subperiods;
3. Use the above procedure to find a good projection (if any);
4. Repeat until a good projection is found.

We easily found several examples using this method. In particular, the following caught our attention because it has very short subperiods. Here are the integer coordinates of these:

$$\begin{aligned} p_0 &= (*, 0, 1, 1), \\ p_1 &= (1, *, -1, 1), \\ p_2 &= (1, -1, *, 0), \\ p_3 &= (2, 1, -1, *), \end{aligned}$$

where $*$ stands for the non-integer coordinate. We checked that there are only two ways to choose these non-integer coordinates so that the subperiods indeed define a plane, namely:

$$\begin{aligned} p_0 &= (a, 0, 1, 1), \\ p_1 &= (1, a - 1, -1, 1), \\ p_2 &= (1, -1, a + 1, 0), \\ p_3 &= (2, 1, -1, a), \end{aligned}$$

with $a = \pm\sqrt{3}$. Proceeding as explained at the beginning of this subsection yields

$$M = \frac{1}{6} \begin{pmatrix} 3 & -a & -a & -2a \\ 0 & a + 3 & a & -a \\ -a & a & -a + 3 & a \\ -a & -a & 0 & 3 \end{pmatrix},$$

whose left kernel is generated, for example, by the rows of the matrix

$$A := \frac{1}{2} \begin{pmatrix} 2 & 0 & a+1 & a-1 \\ 0 & 2 & -a-1 & a+1 \end{pmatrix}$$

Only $a = \sqrt{3}$ defines a valid projection, so we choose this value. We denote by E_c the slope generated by the p_i 's and call **Cyrenaic tilings** the $4 \rightarrow 2$ tilings with slope E_c . Figure 7 illustrates this.

3.3 Defining the prototiles

We describe here the method we used to obtain the tileset \mathcal{C} depicted in Figure 2. Let E be a 2-dimensional irrational plane in \mathbb{R}^4 characterized by its subperiods and which admits a good projection π . Consider a tiling with slope E obtained using the good projection π . Draw through each vertex of this tiling four lines directed by each of the projected subperiods $\pi(p_i)$'s. Figure 8 shows what we obtain for a Cyrenaic tiling. These lines decorate the tiles of the tiling with segments that can take four different directions. All these decorated tiles, considered up to translation, define the wanted tileset. Note that the tileset does not depend on the initially considered tiling, because the $4 \rightarrow 2$ tilings with a given irrational slope share the same finite patterns (this known fact is e.g. proven by Prop. 1 in [BTh17]). Moreover, it is always finite:

Proposition 1 *The tileset obtained by the above method is always finite.*

Proof. We prove that the number of different intervals (distances) between two consecutive lines in a given direction is finite. This yields finitely many ways to decorate a tile by parallel segments, hence finitely many different tiles.

Consider a subperiod p_i and the set \mathcal{D}_i of all lines in E directed by p_i and passing through the vertices of the tiling, i.e by points $\pi(x)$ with $x \in \mathbb{Z}^4 \cap (E + [0, 1]^4)$. Since the distance from a vertex to its neighbors is $\|\pi(e_k)\|$ for some k , the interval between two consecutive lines of \mathcal{D}_i is at most $d_1 := \max_{j \neq i} \{\|\pi(e_j)\|\}$.

Let $\Delta \in \mathcal{D}_i$, $x \in \mathbb{R}^4$ such that $\pi(x) \in \Delta$, and $\Delta' \in \mathcal{D}_i$ which is closest to Δ (Fig. 9). Then the distance from $\pi(x)$ to its orthogonal projection $\pi(x')$ on Δ' is at most d_1 . Besides, the distance between two vertices lying on Δ' is at most $d_2 := \max(\|\pi(\lfloor p_i \rfloor)\|, \|\pi(\lceil p_i \rceil)\|)$. Indeed, if $y \in \mathbb{Z}^4 \cap (E + [0, 1]^4)$ then $y + p_i \in E + [0, 1]^4$ and has three integer coordinates so that it lies on an edge of \mathbb{Z}^4 (seen as a grid in \mathbb{R}^4), between $y + \lfloor p_i \rfloor$ and $y + \lceil p_i \rceil$; now at least one of these two points is in $\mathbb{Z}^4 \cap (E + [0, 1]^4)$, therefore its projection is also a vertex of the tiling, which lies on Δ' (since p_i , $\lfloor p_i \rfloor$ and $y + \lceil p_i \rceil$ are collinear). Hence the distance between $\pi(x')$ and the closest vertex $\pi(y)$ of the tiling which lies on Δ' is at most $d_2/2$.

As a result, $\text{dist}(\pi(x), \pi(y)) \leq d := \sqrt{d_1^2 + d_2^2/4}$, i.e at least one vertex on Δ' is in the ball $B(\pi(x), d)$. Consequently, measuring the intervals around a line Δ in the d -maps of the tiling is enough to list all possible intervals between two consecutive lines in the whole tiling. Since the d -atlas is finite, so is the number

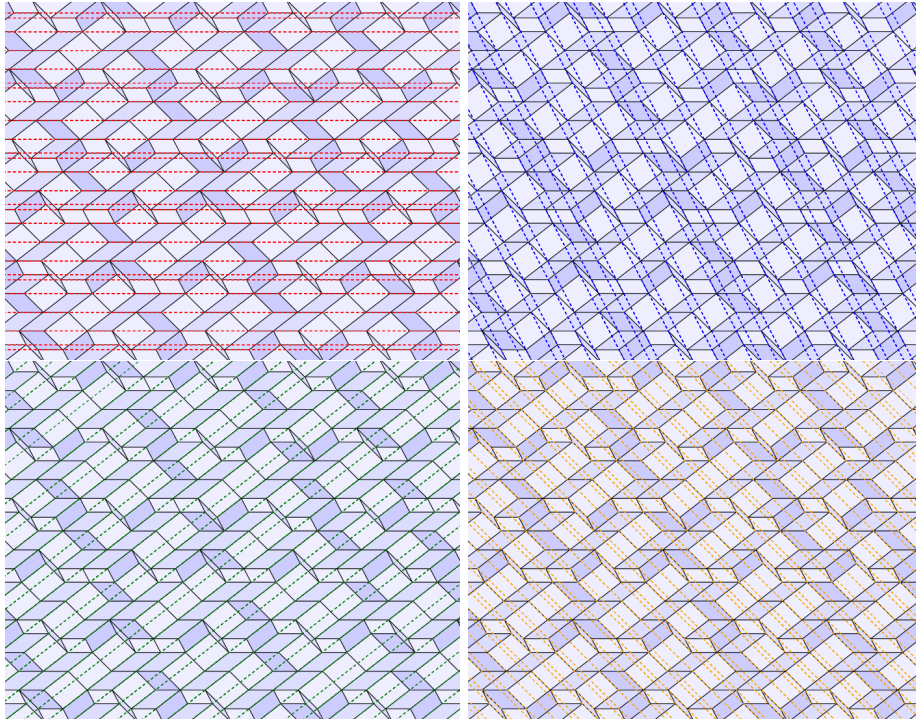


Figure 8: A Cyrenaic tiling with all the lines in the directions of the subperiods, through every vertex of the tiling. Directions are shown separately to ease visualization, and lines are dashed so that one can see the edges of the tiling.

of intervals. □

If the previous proof does not give an explicit bound on the number of tiles, it does give a constructive procedure to obtain these tiles. It is indeed sufficient to compute the constant d (which depends on the subperiods and the projection), then to enumerate the d -maps (for example by enumerating all patterns of size d and keeping only those which can be lifted in a tube $E + [0, 1]^4$ – in practice we used a more efficient algorithm based on the notion of region [BF20] which we do not detail here – and, for each d -map, to draw the lines and enumerate the new decorated tiles obtained. In the case of Cyrenaic tilings, it is sufficient to enumerate the tiles which appear in the 5-atlas in terms of graph distance¹. We obtain 2 or 3 intervals in each direction, and the set \mathcal{C} of 36 decorated prototiles in Figure 2.

¹To get the set \mathcal{C} we used the 6-atlas as a precaution.

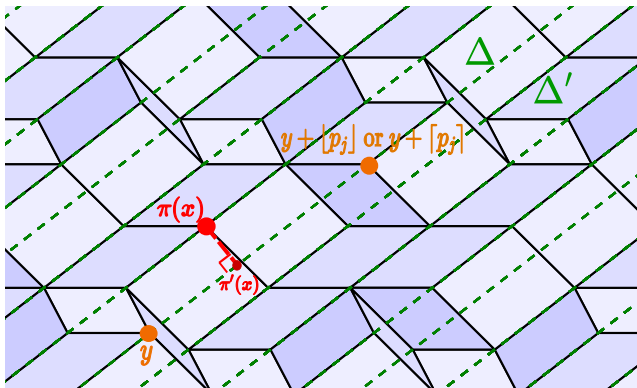


Figure 9: A Cyrenaic tiling with all the lines in the directions of the subperiods, through every vertex of the tiling. Directions are shown separately to ease visualization, and lines are dashed so that one can see the edges of the tiling.

4 Tiling with the tileset \mathcal{C}

By construction, the tileset \mathcal{C} can be used to form all the Cyrenaic tilings (with the decorations by lines). However, nothing yet ensure that these tiles cannot be used to tile in other ways, and obtain for instance tilings which would be periodic or not planar. We shall here prove that this actually cannot happen.

Say we have a set S of tiles decorated with Ammann segments obtained from a given slope $E \subset \mathbb{R}^4$ characterized by subperiods $(p_i)_{i \in \{0,1,2,3\}}$ with a good projection π , and we want to show that any tiling with those tiles is planar with slope E . Let \mathcal{T} be the set of all tilings that can be made with (only) tiles of S . By construction (assembly rules for the tiles in S), four sets of lines appear on any $T \in \mathcal{T}$ and the lines of each set are parallel to a projected subperiod $\pi(p_i)$ and to $\pi(e_i)$ for the same i . We can therefore talk about the i -shadow of T as the tiling obtained when reducing to zero the length of sides of tiles which are parallel to $\pi(p_i)$. Then as shown in Subsection 3.1, for any $i \in \{0, 1, 2, 3\}$, continuity of the lines in direction i is preserved in the i -shadow of T .

Note that this is true for any set of tiles obtained with the method described above. We can then use the lines to show that a shadow is periodic and determine its prime period: starting from a vertex of the shadow, we follow the line in the chosen direction until we hit another vertex, for each valid configuration of the tiles. If the vector from the first vertex to the next is always the same, then it is a prime period of the shadow.

Proposition 2 *Every tiling composed with tiles of \mathcal{C} has the same subperiods as Cyrenaic tilings.*

Proof. For the set \mathcal{C} , we observe that each i -shadow is periodic with period $q_i := \pi_i(p_i)$ where p_i is the i -subperiod of Cyrenaic tilings. This is shown in

Figure 10. In each shadow there are three original (non-decorated) tiles, each of

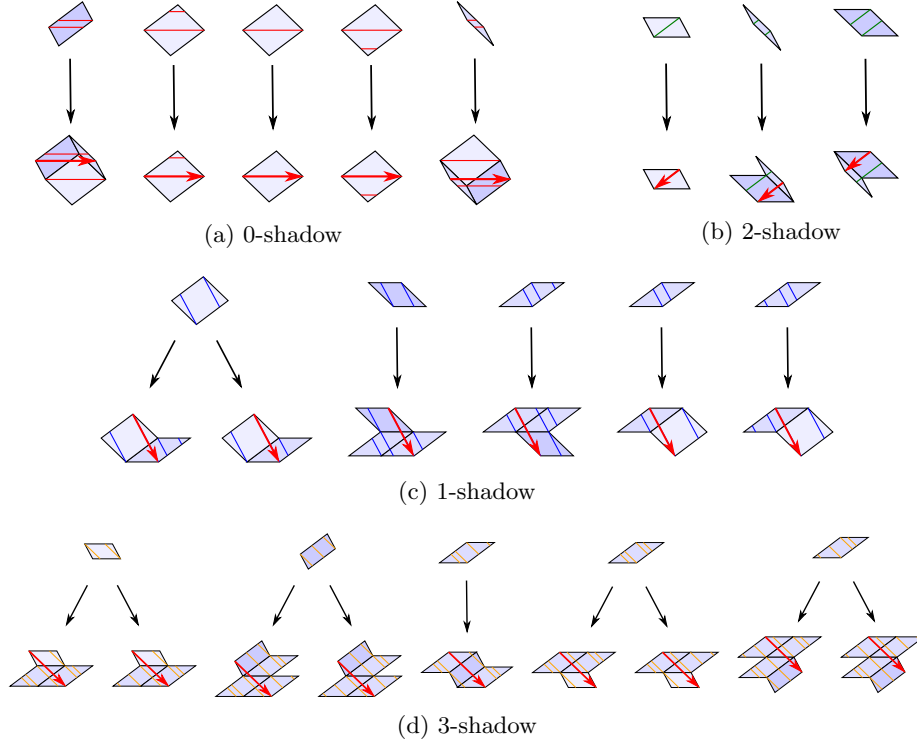


Figure 10: Periods of the 4 shadows of tilings that can be realized with the set \mathcal{C} : starting at any vertex and following a line in direction i , depending on the first traversed tile, there are at most two possibilities until reaching another vertex, and the vector between both vertices is always the same.

which can appear in different versions when taking the decorations into account. For each i -shadow here we only look at the decorations in direction i , where we have the continuity of the lines (other decorations are irrelevant). All possible tiles are given on the top row, and following the arrows from each tile one can see all different possibilities² to place other tiles in order to continue the line directing the red vector. For each shadow, the vector is the same for all possible configurations, which means that the shadow is periodic, and we find exactly the subperiods of Cyrenaic tilings. \square

The main result in [BF15b] thus yields the following:

Corollary 1 *Every tiling composed of tiles of \mathcal{C} is planar with slope E_c .*

There is no guarantee that their thickness is always 1. Yet since the slope E_c is totally irrational, Theorem 1 follows.

²Remember that a line passes through every vertex, in each direction.

Acknowledgements. We would like to thank Alexandre Blondin Massé for his careful proofreading of this article.

A On Ammann bars in Penrose tilings

We present here in more detail the links between Ammann bars and subperiods in Penrose tilings.

A.1 Subperiods

The definition of subperiods is given in Subsection 2.3, here are those of Penrose tilings, which have the form $p_{ij} = (x_0, x_1, x_2, x_3, x_4)$ with $x_i, x_j \in \mathbb{R}$ and $x_k \in \mathbb{Z}$ for $k \notin \{i, j\}$:

$$\begin{aligned} p_{01} &= (1 - \varphi, \varphi - 1, 1, 0, -1), & p_{02} &= (-\varphi, 0, \varphi, 1, -1), \\ p_{03} &= (\varphi, 1, -1, -\varphi, 0), & p_{04} &= (\varphi - 1, 1, 0, -1, 1 - \varphi), \\ p_{12} &= (1, \varphi - 1, 1 - \varphi, -1, 0), & p_{13} &= (1, \varphi, 0, -\varphi, -1), \\ p_{14} &= (0, \varphi, 1, -1, -\varphi), & p_{23} &= (0, 1, \varphi - 1, 1 - \varphi, -1), \\ p_{24} &= (1, -1, -\varphi, 0, \varphi), & p_{34} &= (1, 0, -1, 1 - \varphi, \varphi - 1). \end{aligned}$$

For the following, all indices are in \mathbb{F}_5 (all operations are modulo 5) and we also define some “integer versions” of subperiods, with $i, j \in \{0, 1, 2, 3, 4\}, i < j$:

- “ceiling-floor” $\lceil p_{ij} \rceil$ is p_{ij} with $\lceil x_i \rceil$ in place of x_i and $\lfloor x_j \rfloor$ in place of x_j ,
- “floor-ceiling” $\lfloor p_{ij} \rfloor$ is p_{ij} with $\lfloor x_i \rfloor$ in place of x_i and $\lceil x_j \rceil$ in place of x_j .

Firstly, we observe that for each subperiod, $\pi(\lceil p_{ij} \rceil)$ and $\pi(\lfloor p_{ij} \rfloor)$ have the same direction as $\pi(p_{ij})$ (π denotes the orthogonal projection onto the slope). More precisely,

- the shortest of $\pi(\lfloor p_{i,i+1} \rfloor)$ and $\pi(\lceil p_{i,i+1} \rceil)$ (the first one except for $i = 3$) is equal to $\pi(e_{\min(i-1, i+2)}) - \pi(e_{\max(i-1, i+2)})$ which has the same direction as $\pi(e_i) - \pi(e_{i+1})$ and corresponds to the long diagonal of a thin rhombus, and the other is φ times longer;
- the shortest of $\pi(\lfloor p_{i,i+2} \rfloor)$ and $\pi(\lceil p_{i,i+2} \rceil)$ is equal to $\pm\varphi(\pi(e_i) - \pi(e_{i+2}))$ which corresponds to the short diagonal of a thick rhombus, and the other is φ times longer (which corresponds to the long diagonal of a thick rhombus).

For instance, $\lfloor p_{14} \rfloor = (0, 1, 1, -1, -1)$, $\lceil p_{14} \rceil = (0, 2, 1, -1, -2)$, and for $a \in \mathbb{R}$ we have

$$(0, 1 + a, 1, -1, -(1 + a)) = ae_1 + (e_1 + e_2) - (e_3 + e_4) - ae_4$$

Hence, since $\pi(e_i + e_{i+1}) = -\varphi\pi(e_{i-2})$ for all $i \in \mathbb{F}_5$,

$$\begin{aligned} \pi(0, 1 + a, 1, -1, -(1 + a)) &= a\pi(e_1) - \varphi\pi(e_4) + \varphi\pi(e_1) - a\pi(e_4) \\ &= (\varphi + a)(\pi(e_1) - \pi(e_4)) \end{aligned}$$

Thus for $a = 0, \varphi - 1, 1$ we obtain that $\pi(\lfloor p_{14} \rfloor)$, $\pi(p_{14})$ and $\pi(\lceil p_{14} \rceil)$ are collinear. Only the order of coordinates changes for other subperiods.

A.2 Link with Ammann bars

Firstly, directions of the subperiods are the same as directions of the Ammann bars, $\pi(p_{ij})$ being orthogonal to $\pi(e_i) + \pi(e_j)$. For instance, $p_{01} \perp e_3$ and we have $\pi(e_0) + \pi(e_1) = -\varphi\pi(e_3)$ since the long diagonal of a thick rhombus is φ times longer than the side. Figure 1 illustrates these relations, which are the same in every direction up to rotation: it shows part of a Penrose tiling with Ammann bars as well as $\lfloor p_{ij} \rfloor$ and $\lceil p_{ij} \rceil$ for one subperiod. Moreover, when the side of a tile has length φ , on the one hand the “distances” between Ammann bars of a given set, measured not orthogonally but with an angle of $\frac{2\pi}{5}$ rad = 72 degrees, are $S = 2 \sin \frac{2\pi}{5}$ and $L = \varphi S$; and on the other hand the norms of $\pi(\lceil p_{i,i+1} \rceil)$ and $\pi(\lfloor p_{i,i+1} \rfloor)$ are L and $S + L = \varphi L$ i.e. φ times longer (the long diagonal of a thin rhombus has length L).

Remark 1 *There is exactly one Ammann segment in every direction in each tile. Hence taking into account the distances between consecutive bars, respecting conditions on Ammann bars forces subperiods.*

B Details about computations

Reading this appendix is not necessary to understand the article but may be of interest to readers who find that too many calculations are swept under the rug. Some of these calculations are difficult and rely on functions that we wrote using SageMath (Python with classical mathematical functions that are very useful here). All these functions can be found in the ancillary file `code.sage` of the ArXiv file. The purpose of this appendix is to explain how these functions work.

B.1 Computing cut and project tilings

We use the duality between *multigrids* [dB81] and cut and project tilings. A *grid* is a set of regularly spaced parallel hyperplanes (lines in the case of an $n \rightarrow 2$ tiling). A multigrid is then a $d \times n$ matrix G whose rows define the direction and spacing of each grid (normal vector to each hyperplane, with the norm giving the spacing), and a *shift vector* S which specifies how each grid is translated away from the origin. The shift must be chosen such that no more than d hyperplanes intersect in a point (this is generic).

The function `generators_to_grid(E)` convert a slope E , given by d vectors of \mathbb{R}^n which generate it, to a multigrid G .

Then, to each intersection of d hyperplanes corresponds a tile: it is generated by the directions of the hyperplanes, and the i -th coordinate of its position is the number of hyperplane in the i -th direction between the origin and the considered intersection.

The function $\text{dual}(G, S, k)$ computes the *dual* of the multigrid G with shift vector S and $2k + 1$ grids in each direction (since we can only compute a subset of the infinite tiling). This is a set of tiles represented each by a pair (t, pos) where t is the d -tuple of indices of the vectors of the standard basis which define the prototile and pos is the integer translation applied on it (in \mathbb{Z}^n).

B.2 Finding the integer entries of a subperiod

Consider a slope E generated by the vectors $u_1, \dots, u_d \in \mathbb{R}^n$. We assume that the entries of the u_i 's are in $\mathbb{Q}(a)$ for some algebraic number a , because it has been proven in [BF20] to be a necessary condition to have local rules. We want to find a subperiod p of E , that is a vector of E with $d + 1$ integer coordinates – the *type* of p gives us the indices of its integer coordinates $a_{i_1}, \dots, a_{i_{d+1}}$ ($1 \leq i_1 < i_2 < \dots < i_{d+1} \leq n$). For this, we consider the $n \times (d + 1)$ matrix N whose columns are the u_j 's and the subperiod p to be determined:

$$N = \left(\begin{array}{c|c|c|c|c} \cdot & \cdot & \cdots & \cdot & \cdot \\ \cdot & \cdot & \cdots & \cdot & a_{i_1} \\ & & & & a_{i_2} \\ & & & & \vdots \\ u_1 & u_2 & \cdots & u_d & p \\ \cdot & \cdot & \cdots & \cdot & a_{i_k} \\ & & & & \vdots \\ \cdot & \cdot & \cdots & \cdot & a_{i_{d+1}} \\ & & & & \cdot \end{array} \right)$$

Since $p \in E$, this matrix has rank d and all the $(d + 1)$ -minors are thus zero. In particular, the nullity of the minor obtained by selecting the lines i_1, \dots, i_d yields a linear equation on the a_{i_k} . Indeed, developing the minor along the last column yields

$$(a_{i_1}, \dots, a_{i_{d+1}}) \times \begin{pmatrix} (-1)^1 G_{i_2 \dots i_{d+1}} \\ \vdots \\ (-1)^k G_{i_1 \dots \widehat{i_k} \dots i_{d+1}} \\ \vdots \\ (-1)^{d+1} G_{i_1 \dots i_d} \end{pmatrix} = 0,$$

where $G_{i_1 \dots \widehat{i_k} \dots i_{d+1}}$ is the determinant of the $d \times d$ matrix obtained by taking the coordinates i_1, \dots, i_{d+1} except i_k of the u_i 's (it is also known as *Grassmann coordinates* of the plane). Since the a_i 's must be integer, this can equivalently be rewritten as follows. Replace each coefficient $(-1)^k G_{i_1 \dots \widehat{i_k} \dots i_{d+1}}$ by a line of length $\deg(a)$, the algebraic degree of a , whose i -th entry is the coefficient of a^i in $(-1)^k G_{i_1 \dots \widehat{i_k} \dots i_{d+1}}$. This yields a $n \times \deg(a)$ integer matrix. Then, the a_i 's are obtained by computing the left kernel of this matrix.

The above algorithm is implemented in the function `subperiods(E)`, which outputs a list of subperiods represented each by its type and its $d + 1$ integer entries.

Let us illustrate this with the Cyrenaic tiling. The slope E is generated by the lines of the matrix

$$\begin{pmatrix} a & 0 & 1 & 1 \\ 1 & a-1 & -1 & 1 \end{pmatrix},$$

where $a = \sqrt{3}$. Let us search a subperiod whose first three entries are integer. The matrix N is

$$N = \begin{pmatrix} a & 1 & a_1 \\ 0 & a-1 & a_2 \\ 1 & -1 & a_3 \\ 1 & 1 & * \end{pmatrix},$$

where $*$ denotes the non-integer entry we are here not interested in. Consider the 3-minor obtained with the three first lines and develop it along the last column. We get:

$$(a_1, a_2, a_3) \times \begin{pmatrix} -a+1 \\ a+1 \\ -a+3 \end{pmatrix} = 0.$$

Since $a = \sqrt{3}$, $\deg(a) = 2$ and this is equivalent to

$$(a_1, a_2, a_3) \times \begin{pmatrix} -1 & 1 \\ 1 & 1 \\ -1 & 3 \end{pmatrix} = 0.$$

This 3×2 integer matrix turns out to have rank 2. Its left kernel has dimension 1 and the a_i 's are given by a prime integer vector in this kernel:

$$(a_1, a_2, a_3) = (2, 1, -1).$$

This yields the subperiod $p_3 = (2, 1, -1, *)$, as claimed in Subsection 3.2.

B.3 Determining whether a slope is characterized by its subperiods

To determine whether a slope E is characterized by its subperiods, we first compute the subperiods of E as explained in the previous subsection. Then, we form the matrix whose columns are these subperiods, with variables x_i 's for the non-integer coordinates (since only the integer coordinates are known). Since these subperiods must belong to the d -dimensional plane E , any $(d + 1)$ -minor of this matrix must be zero. This yields an equation. By considering all the minors, we get a system of polynomial equation. The slope is characterized by its subperiods if and only if this system has dimension zero.

This is implemented in the function `is_determined_by_subperiods(E)`.

B.4 Finding the non-integer entries of a subperiod

To compute the subperiods of a slope E seen as vectors in E , we first compute the integer entries of the subperiods as explained above. We then consider the unknown non-integer entries as variables x_i 's. The matrix formed by the subperiods has rank d since all the subperiods must be in the d -dim. plane E . Its $(d + 1)$ -minors must thus all be zero. This yields a polynomial system of equations in the x_i 's. We take the solution which is in E : this yields all the coordinates of the subperiods.

This is implemented in the function `lifted_subperiods(E)`.

B.5 Finding a good projection

The method to find a good projection is described in Subsection 3.2. It is implemented by the function `good_projection(E)`. We also implemented the function `valid_projection(A,E)`, which checks whether the projection A is valid for the slope E .

B.6 Computing the r -atlas

Computing the r -atlas of a cut and project tiling mainly relies on the notions of *window* and *region*. We here briefly recall these notions; the interested reader can find more details in [BF20].

Consider a strongly planar $n \rightarrow d$ tiling with a given slope E . Consider the simplest pattern: a single edge directed by $\pi(e_i)$. To decide whether this pattern appears somewhere in the tiling, we have to decide whether there exists a vertex x of the tiling such that $x + \pi(e_i)$ is also a vertex of the tiling. By definition, a vertex x belongs to the tiling if and only if its lift \hat{x} belongs to the tube $E + [0, 1]^n$. The idea is to look in the space orthogonal to E , denoted by E' (sometimes called *internal space*, while E is called *real space*). Denote by π' the orthogonal projection onto E' . Now, a vertex x belongs to the tiling iff $\pi'(\hat{x})$ belongs to the polytope $W := \pi'([0, 1]^n)$. This polytope is called the *window* of the tiling. Similarly, $x + \pi(e_i)$ belongs to the tiling iff $\pi'(\hat{x} + e_i)$ belongs to W , that is, iff $\pi'(\hat{x})$ belongs to $W - \pi'(e_i)$. Hence, there exists two vertices x and $x + \pi(e_i)$ of the tiling if and only if the following polytope is not empty:

$$R(e_i) := W \cap (W - \pi'(e_i)).$$

The polytope $R(e_i)$ is called the *region* of the pattern formed by a single edge directed by $\pi(e_i)$. This can be extended to any pattern P : such a pattern appears somewhere in the tiling iff its region, defined as follows, is not empty:

$$R(P) := \bigcap_{x \in P} W - \pi'(\hat{x}),$$

where the intersection is taken over the vertices of P . This is easily implemented in the function `region(W,ip,P)`, which takes as parameter the window, the internal projection and the pattern.

Let us now explain how to use regions to compute the r -atlas. We shall maintain a list of the already computed r -maps, together with their regions in the window W . We start with an empty list and fill it progressively as follows.

While the already computed regions do not cover the whole W , we first pick at random a point z in W which is not in one of the already computed region. We then associate with z the set of points $u \in \mathbb{Z}^n$ with norm at most r such that $z + \pi' u \in W$. This set is an r -map, which is new because its region does not overlap the already computed regions. We compute the region of this r -map and we add both the map and the region in our list.

There is an additional tricky minor detail. Before computing the region of an r -map, we must “close” this r -map, that is, add the tiles that are forced by the r -map: whenever two consecutive segments on the boundary of the pattern form a notch where a single tile can be added, then we must add this tile (because we know that there is no other segments dividing this notch - the information that there is nothing is indeed an information on its own).

All this is implemented in the function `atlas(E,r)`, which use two auxiliary functions.

B.7 Computing the decorated tiles

To compute the decorated tiles, we first compute a sufficiently large atlas (in the case of the Cyrenaic tilings the 6-atlas is sufficient). Then, for each pattern in this atlas, we compute the lines directed by the subperiods which go through each vertex of the pattern and intersect them with the tile at the origin of the pattern: this yields one decorated tile. This is implemented in the function `decorated_tile`. We proceed similarly for each pattern of the atlas (function `decorated_tiles`) to get the whole decorated tileset.

References

- [Bee82] F. P. M. Beenker. Algebraic theory of non periodic tilings of the plane by two simple building blocks: a square and a rhombus. Technical Report TH Report 82-WSK-04, Technische Hogeschool Eindhoven, 1982.
- [Ber66] R. Berger. *The Undecidability of the domino problem*. American Mathematical Society, 1966.
- [BF13] N. Bédaride and Th. Fernique. The Ammann–Beenker tilings revisited. In Siegbert Schmid, Ray L. Withers, and Ron Lifshitz, editors, *Aperiodic Crystals*, pages 59–65, Dordrecht, 2013. Springer Netherlands.
- [BF15a] N. Bédaride and Th. Fernique. No weak local rules for the 4p-fold tilings. *Discrete & Computational Geometry*, 54(4):980–992, Oct 2015.

- [BF15b] N. Bédaride and Th. Fernique. When periodicities enforce aperiodicity. *Communications in Mathematical Physics*, 335(3):1099–1120, Feb 2015.
- [BF20] N. Bédaride and Th. Fernique. Canonical projection tilings defined by patterns. *Geometriae Dedicata*, 208(1):157–175, feb 2020.
- [BTh17] N. Bédaride and Fernique Th. Weak local rules for planar octagonal tilings. *Israel Journal of Mathematics*, 222(1):63–89, Oct 2017.
- [Bur88] S. E. Burkov. Absence of weak local rules for the planar quasicrystalline tiling with the 8-fold rotational symmetry. *Communications in Mathematical Physics*, 119(4):667–675, 1988.
- [dB81] N. G. de Bruijn. Algebraic theory of Penrose’s non-periodic tilings of the plane. *Mathematics Proceedings*, A84:39–66, 1981. Reprinted in [SO87].
- [Gar77] M. Gardner. Mathematical games. *Scientific American*, 236(1):110–121, 1977.
- [GS87] B. Grünbaum and G. C. Shephard. *Tilings and Patterns*. W. H. Freeman and Company, New York, 1987.
- [Har04] E. O. Harriss. *On Canonical Substitution Tilings*. PhD thesis, University of London, 2004.
- [Lev88] L. Levitov. Local rules for quasicrystals. *Communications in Mathematical Physics*, 119:627–666, 1988.
- [PBM20] C. Porrier and A. Blondin Massé. The Leaf function of graphs associated with Penrose tilings. *International Journal of Graph Computing*, 1.1:1–24, 2020.
- [Pen74] R. Penrose. The role of aesthetics in pure and applied mathematical research. *Bulletin of the Institute of Mathematics and its Applications*, pages 266–271, 1974. Reprinted in [SO87].
- [Pen78] R. Penrose. Pentaplexity. *Math. Intelligencer*, 2(1):32–37, 1978.
- [Sen95] M. Senechal. *Quasicrystals and Geometry*. Cambridge University Press, 1995.
- [Sen04] M. Senechal. The Mysterious Mr. Ammann. *The Mathematical Intelligencer*, 26:10–21, 2004.
- [SO87] P. J. Steinhardt and . Ostlund, editors. *The Physics of Quasicrystals*. World Scientific, 1987. Collection of reprints. ISBN 9971-50-226-7.
- [Soc89] J. E. S. Socolar. Simple octagonal and dodecagonal quasicrystals. *Phys. Rev. B*, 39:10519–10551, 1989.